# Ni spin switching induced by magnetic frustration in FeMn/Ni/Cu(001)

J. Wu,[1] J. Choi,[1] A. Scholl,[2] A. Doran,[2] E. Arenholz,[2] Chanyong Hwang,[3] and Z. Q. Qiu[1]

[1]Department of Physics, University of California Berkeley, Berkeley, CA 94720
[2]Advanced Light Source, Lawrence Berkeley National Laboratory, Berkeley, CA 94720
[3]Division of Advanced Technology, Korea Research Institute of Standards and Science, 209 Gajeong-Ro, Yuseong-Gu, Daejeon 305-340, Korea

Abstract

Epitaxially grown FeMn/Ni/Cu(001) films are investigated by Photoemission Electron Microscopy and Magneto-Optic Kerr Effect. We find that as the FeMn overlayer changes from paramagnetic to antiferromagnetic state, it could switch the ferromagnetic Ni spin direction from out-of-plane to in-plane direction of the film. This phenomenon reveals a new mechanism of creating magnetic anisotropy and is attributed to the out-of-plane spin frustration at the FeMn-Ni interface.

PACS numbers: 75.70.Ak

Controlling the local electron spin direction in a magnetic nanostructure is a key step towards spintronics applications [1]. Various methods have been proposed to reach this goal in the last decades such as the spatial variation of the g-factor [2], tuning of the charge density [3], spin torque effect [4,5], and the voltage-controlled multiferroic antiferromagnet [6], etc. Since the direct spin-spin dipolar interaction is rather weak in solids (~$10^{-4}$ eV), all approaches are to some extend based on the spin-charge interaction to modify the electronic orbits that are coupled to the electron spins. For magnetic materials, such spin-charge interaction often manifests as the spin-orbit coupling which generates the so-called magnetic anisotropy to determine the electron spin direction, i.e. the easy magnetization axis. Therefore a control of the local electron spin direction is ultimately related to the manipulation of the magnetic anisotropy. For example, controlling the spins both along the surface normal and in the surface plane of a magnetic thin film has been realized by tailoring surface and step-induced magnetic anisotropies [7,8,9]. Although research on the magnetic anisotropy has been greatly advanced in the last decades, its limitation is that once a magnetic nanostructure is synthesized the interfacial electronic states are fixed and it is very difficult to change the magnetic anisotropy. Then the interesting question arises if new mechanisms exist that could generate a magnetic anisotropy? Exploring such new mechanisms would be obviously important to the development of spintronics technology. In this Letter, we demonstrate a new way to switch the spin direction of a ferromagnetic thin film. We show that the spin direction of a Ni thin film in FeMn/Ni/Cu(001) can be switched from parallel to the surface normal into the surface plane of the film by changing the magnetic state of the antiferromagnetic FeMn layer. We show that this phenomenon is due to the magnetic frustration at the FeMn/Ni interface which generates a magnetic anisotropy shifting the Ni spin reorientation transition (SRT) thickness [10] by as much as 40%. We choose this system because FeMn/Ni/Cu(001) films can be grown epitaxially and FeMn has a well-defined 3Q antiferromagnetic spin structure so that well-defined single crystalline ultrathin films can be synthesized for this study with the FeMn Néel temperature easily tuned by changing its film thickness [11].

A 10 mm diameter Cu(001) single crystal disk was mechanically polished down to 0.25 μm diamond-paste, followed by an electropolish [12]. The substrate was cleaned

*in situ* by cycles of $Ar^+$ sputtering at 2-5 keV and annealing at 600-700°C. FeMn/Ni/Cu(001) films were grown at room temperature with a base pressure below $3\times10^{-10}$ Torr. The FeMn and Ni films were grown into wedges oriented at 90º to each otherin order to evaluate the impact of their thickness on the magnetic properties of the system independently. The FeMn film was grown by coevaporating Fe and Mn with equal evaporation rates leading to a 50-50 composition. A 10 ML Cu layer was grown on top of the FeMn to protect the sample from contamination. Magnetic properties of the films were measured by Magneto-Optic Kerr Effect (MOKE) using a He-Ne laser (beam diameter 0.2 mm) and by Photoemission Electron Microscopy (PEEM) at the Advanced Light Source of Lawrence Berkeley National Laboratory. The magnetic contrast was obtained by taking the ratio of images obtained at the $L_3$ and $L_2$ edges utilizing x-ray magnetic circular dichroism (XMCD) [13]. All measurements were made at room temperature.

We first present Ni domain images (Figure 1) of FeMn/Ni/Cu(001) at a fixed Ni thickness of 8.2 ML as a function of the FeMn overlayer thickness. The Ni domains exhibit two different levels of contrast below 7.5 ML of FeMn ($d_{FeMn}$<7.5 ML) and multiple levels of contrast above 7.5 ML of FeMn. After rotating the sample by 90º around its surface normal, the Ni domain contrast remains unchanged for $d_{FeMn}$<7.5 ML but changes for $d_{FeMn}$>7.5 ML. Recalling that the Ni domain contrast originates from the XMCD signal that is determined by the angle between the incident x-ray and the local spin direction, we conclude that the Ni magnetization in Figure 1 is perpendicular to the film plane for $d_{FeMn}$<7.5 ML and in the film plane for $d_{FeMn}$>7.5 ML, i.e., the FeMn/Ni(8.2ML)/Cu(001) films undergo a spin reorientation transition (SRT) at 7.5 ML of FeMn thickness. Note that in the conventional SRT in Ni/Cu(001) the Ni spin direction turns from in-plane to out-of-plane with increasing the Ni film thickness [14]. In our case, the Ni film thickness is actually fixed at 8.2ML so that the SRT in Figure 1 is induced by the FeMn overlayer rather than by the Ni film itself. On the other hand, the Ni spin direction is ultimately determined by its overall magnetic anisotropy. Figure 1 shows that the FeMn film must have induced a magnetic anisotropy to the Ni film. This implies that different FeMn thicknesses should lead to different Ni conventional SRT as a function of Ni film thickness. To verify this hypothesis, we show in Figure 2 the Ni

PEEM images as a function of the Ni film thickness at fixed FeMn thicknesses of 5.7 ML and 8.4 ML, respectively. For each case, the Ni film shows an in-plane to out-of-plane SRT with increasing the Ni thickness as in the Ni/Cu(001) system. However, the Ni SRT critical thickness of $d_{SRT}$=10.5 ML for $d_{FeMn}$=8.4 ML sample is about 40% greater than the Ni SRT thickness of $d_{SRT}$=7.5 ML for $d_{FeMn}$=5.7 ML sample, confirming that the thicker FeMn ($d_{FeMn}$>7.5 ML) must have induced a magnetic anisotropy which favors the Ni spins parallel to the film plane. Since both FeMn(5.7ML)/Ni/Cu(001) and FeMn(8.4ML)/Ni/Cu(001) samples have the same FeMn/Ni interface and the interfacial magnetic anisotropy depends little on the overlayer thickness above 5ML [15], the different Ni SRT thickness shown in Figure 2 must be induced by a change in the magnetic state of the FeMn film. Since the Néel temperature of the FeMn film increases with its film thickness, we attribute the FeMn induced magnetic anisotropy to the antiferromagnetic order of the FeMn overlayer. To support this conclusion, we determined the Ni SRT thickness $d_{SRT}$ systematically from PEEM images at different FeMn thicknesses to construct a phase diagram in the $d_{Ni}$-$d_{FeMn}$ thickness plane (Figure 3). The $d_{SRT}$ remains a constant of 7.5 ML for $d_{FeMn}$ < 7 ML, exhibits a sudden increase for 7 ML < $d_{FeMn}$ <8 ML, and reaches another constant value of 10.5 ML for $d_{FeMn}$ > 8 ML. Then the constant Ni $d_{SRT}$ values for $d_{FeMn}$ < 7 ML and $d_{FeMn}$ > 8 ML correspond to the paramagnetic and antiferromagnetic states of the FeMn films at room temperature. The critical thickness of $d_{FeMn}$=7.5 ML at room temperature is similar to the literature value of $d_{FeMn}$~9-10 ML for FeMn/Co system [16,17].

To further confirm our conclusion, polar MOKE hysterisis loops, which measure the Ni perpendicular magnetization, were detemined as function of both the Ni thickness at different magnetic state of the FeMn overlayer at room temperature. Figure 4(a) show the Ni polar loops at paramagnetic ($d_{FeMn}$=4.3 ML) and antiferromagnetic ($d_{FeMn}$=9.7 ML) state of the FeMn film, respectively. In both cases, the Ni film develops the polar signal above a critical thickness to eventually evolve into a square loop with a full remanence, indicating the Ni SRT from in-plane to out-of-plane directions with increasing the Ni thickness. However, there are two major differences. First, the Ni SRT critical thickness is thinner at paramagnetic FeMn [left column of Figure 4(a)] than at antiferromagnetic FeMn [right column in Figure 4(a)]. To illustrate this aspect, the Ni polar remanence (M

□) is plotted as a function of the Ni thickness [Figure 4(b)] for $d_{FeMn}$=4.3 ML and 9.7 ML, respectively. It is clearly seen that the Ni SRT thickness [indicated by arrows in Figure 4(b)] is $d_{SRT}$=7.5 ML at $d_{FeMn}$=4.3 ML and $d_{SRT}$=10.5 ML at $d_{FeMn}$=9.7 ML, in agreement with the PEEM result. Second, it is obvious that the coercivity ($H_C$) of the Ni hysterisis loops is much larger for antiferromagnetic FeMn than for paramagnetic FeMn. To obtain a detailed dependence of the Ni coercivity on the FeMn thickness, we measured polar MOKE loops at a fixed Ni thickness of 14.5 ML and determined the coercivity as a function of the FeMn thickness. The result [Figure 4(c)] shows that $H_C$ remains a constant value below an FeMn critical thickness of $d_{FeMn}$=7.5 ML and then increases rapidly above the FeMn critical thickness. The drastic increase of $H_C$ above an FeMn critical thickness in FeMn/ferromagnetic bilayers is a strong evidence for the establishment of the antiferromagnetic order in the FeMn film [18]. This confirm our conclusion that it is the antiferromagnetic order of the FeMn overlayer that induces a magnetic anisotropy to the Ni film.

To understand how the FeMn antiferromagnetic order induces a magnetic anisotropy, we consider the spin structure of the face centered cubic (fcc) FeMn lattice. The fcc antiferromagnetic FeMn has a nonlinear 3Q-like spin structure [Figure 5(a)][19], giving rise to a zero total spin per tetrahedral unit cell. For FeMn (001) atomic planes, although the in-plane net spin is zero, the out-of-plane net spin is nonzero but alternating its direction between neighboring (001) planes. Then at the FeMn/Ni interface with atomic steps (inevitable in real experimental systems), this kind of 3Q spin structure will give rise to (1) a nonzero perpendicular net spin at each atomic terrace whose direction alternates between neighboring terraces [Figure 5(b)], and (2) a net in-plane spin component present only at the [100]-type step edges [Figure 5(c)][11]. For the perpendicular FeMn spin component, the FeMn/Ni magnetic coupling will produce a magnetic frustration due to the presence of atomic steps [20]: the FeMn-Ni interfacial interaction favors an alternating alignment of the Ni spins between neighboring terraces while the Ni-Ni ferromagnetic interaction prefers a parallel alignment of the Ni spins. This magnetic frustration is similar to the case of the biquadratic interlayer coupling in magnetic sandwiches [21] and the 90-degree coupling at the FM/AFM interfaces [22] where the AF and FM couplings compete witheach other. The result of this competition

is to generate a uniaxial magnetic anisotropy which favors a perpendicular alignment of the FM spins to the AF spins, similar to the well-known "spin-flop" state in bulk antiferromagnets [23]. For the case of FeMn/Ni/Cu(001), the FeMn/Ni out-of-plane interfacial magnetic frustration should generate a magnetic anisotropy that favors the Ni spins to be perpendicular to the film normal direction. This is consistent with our observation that the antiferromagnetic order of the FeMn overlayer favors the Ni spins to be in the film plane. For the effect of the in-plane component of the FeMn spins, the uncompensated spins at the [±1,0,0] and [0,±1,0] step edges should create an equivalent four-fold magnetic anisotropy for the in-plane magnetization of the Ni film [11] which could also favor an in-plane alignment of the Ni spins.

Which of the above two mechanisms, out-of-plane or in-plane FeMn component, is responsible for our observations? To answer this question, we performed an additional experiment on FeMn/Ni films grown on vicinal Cu(001) substrate with the steps parallel to [100] direction. The idea is that the interfacial frustration due to the FeMn out-of-plane spin component should scale with the terrace width so that the magnetic anisotropy energy per unit area should be weakly dependent on the step density. On the other hand, the effect due to the in-plane FeMn uncompensated spin component at the [100]-step edges should obviously increase with the [100] step density. Therefore a study of the Ni SRT thickness as a function of the vicinal angle (step-density) should be able to distinguish these two mechanisms. A half-flat/half-curved Cu(001) substrate is used in our experiment to change the vicinal angle ($\alpha$) continuously from $0^o$ to $10^o$ [24]. The formation of the regular [100] atomic steps on the curved substrate is verified by a clear splitting of the diffraction spots in the Low Energy Electron Diffraction (LEED). After the deposition of a Ni wedge with its slope along the [100] step direction and a uniform FeMn film, MOKE measurement is carried out at room temperature to determine the Ni SRT thickness $d_{SRT}$. Figure 6 shows the result of $d_{SRT}$ as a function of the vicinal angle $\alpha$ for paramagnetic ($d_{FeMn}$=5 ML) and antiferromagnetic ($d_{FeMn}$=17 ML) FeMn overlayers. The purpose of including the paramagnetic FeMn case is to identify possible effect of the step-induced magnetic anisotropy on the Ni SRT [25]. We find that for paramagnetic FeMn ($d_{FeMn}$=5 ML), the $d_{SRT}$ value of 7.5ML is independent of $\alpha$, showing that we can ignore the effect of the step-induced magnetic anisotropy on the Ni SRT. As the FeMn

film becomes antiferromagnetic at thicker thickness ($d_{FeMn}$=17 ML), the Ni $d_{SRT}$ value shifts from 7.5 ML to 10.5 ML, showing the effect of the FeMn-Ni interfacial frustration on the Ni SRT. More importantly, the Ni SRT thickness remains a constant value of $d_{SRT}$=10.5 ML with increasing the vicinal angle $\alpha$ shows that the FeMn uncompensated in-plane spins at the [100]-step edges have little effect on the Ni SRT. Then the result of Figure 6 proves that it is the FeMn out-of-plane spin component that is responsible for the FeMn induced magnetic anisotropy. Taking the 3 ML Ni SRT thickness shift and the Ni magnetic anisotropy value in Ni/Cu(001) system [10], we estimate the strength of this frustration induced magnetic anisotropy to be ~70 μeV/spin, the same order of magnitude as estimated by Koon [22]. We would also like to point out that this frustration induced SRT should be a general phenomenon as far as the crystal plane of the film surface carries an uncompensated net spins whose direction alternates between neighboring terraces. Finally, another interesting topic for future study could be the exchange bias in this system because the unidirectional and uniaxial magnetic anisotropies due to the FeMn-Ni interfacial interaction are in two different directions.

In summary, we studied the Ni spin reorientation transition in FeMn/Ni/Cu(001) system and find a 40% Ni SRT thickness shift as the FeMn overlayer transits from paramagnetic to antiferromagnetic state. We attribute this giant shift to the out-of-plane FeMn-Ni interfacial magnetic frustration which generates a magnetic anisotropy to the Ni film.

**Acknowledgement**

This work was supported by National Science Foundation DMR-0803305, U.S. Department of Energy DE-AC02-05CH11231, ICQS of Chinese Academy of Science, and KICOS through Global Research Laboratory project. The Advanced Light Source is supported by the Director, Office of Science, Office of Basic Energy Sciences, of the U.S. Department of Energy under Contract No. DE-AC02-05CH11231.

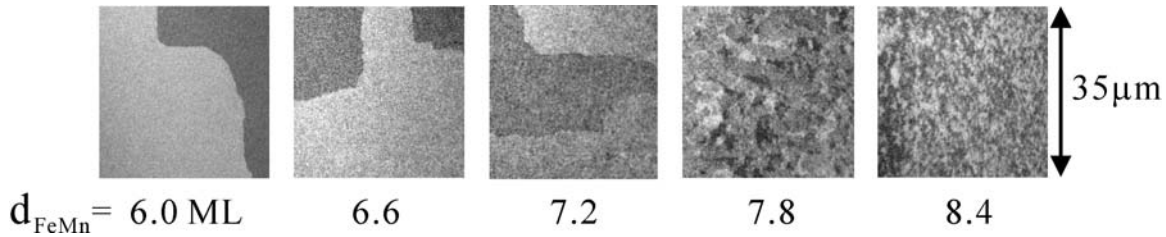


Fig. 1: Ni domain images of FeMn/Ni(8.2ML)/Cu(001) as a function of the FeMn overlayer thickness. The antiferromagnetic order of FeMn overlayer above 7.5ML switches the Ni spin from out-of-plane to in-plane direction of the film.

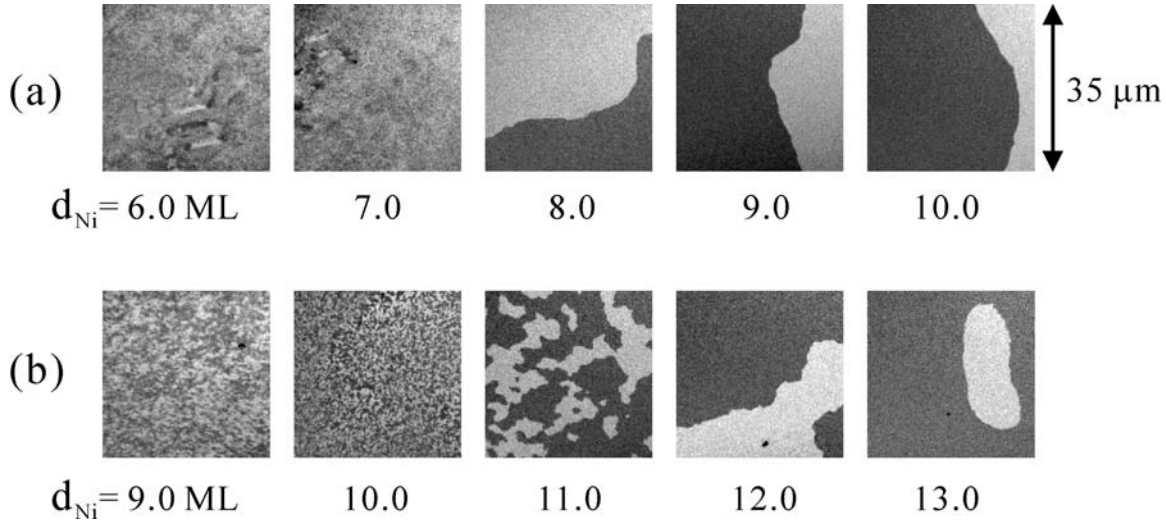


Fig. 2: Ni domain images of FeMn/Ni/Cu(001) as a function the Ni film thickness. The Ni spin reorientation transition takes place (a) at $d_{SRT}$=7.5ML for paramagnetic FeMn overlayer ($d_{FeMn}$=5.7 ML), and (b) at $d_{SRT}$=10.5ML for antiferromagnetic FeMn overlayer ($d_{FeMn}$=8.4 ML).

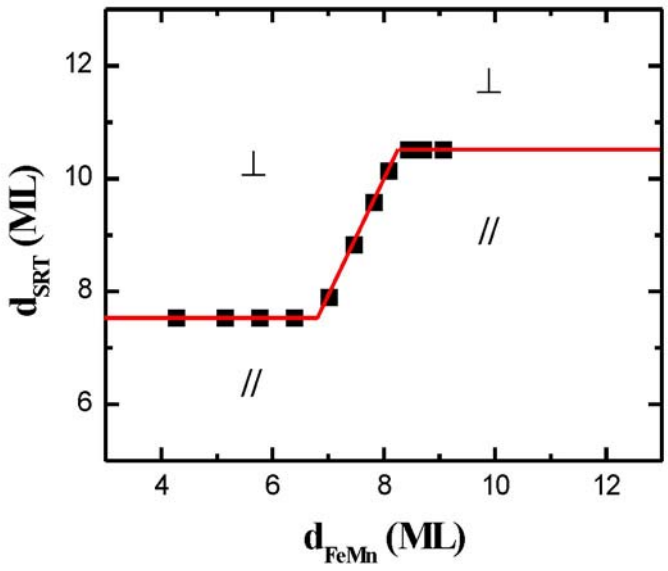


Fig. 3: (color online) The Ni SRT critical thickness $d_{SRT}$ as a function of $d_{FeMn}$. The red solid line is guide to eyes. The antiferromagnetic order of the FeMn film above 7.5ML generates a magnetic anisotropy to increases the Ni SRT from 7.5ML to 10.5 ML.

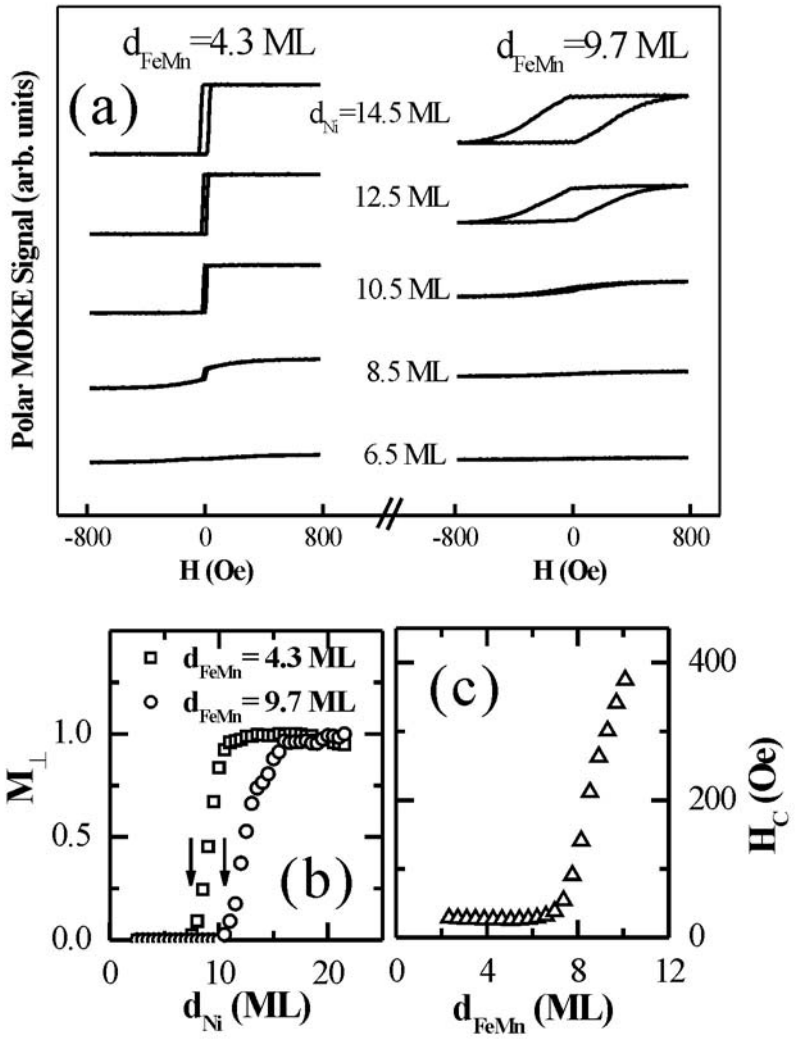


Fig. 4: (a) Polar MOKE hysterisis loops of FeMn/Ni/Cu(001) as a function of Ni thickness for paramagnetic FeMn overlayer (left column, $d_{FeMn}$=4.3 ML), and antiferromagnetic FeMn overlayer (right column, $d_{FeMn}$=8.4 ML). (b) The Ni polar remanence as a function of Ni film thickness. (c) The coercivity of FeMn/Ni(14.5ML)/Cu(001) as a function of the FeMn film thickness.

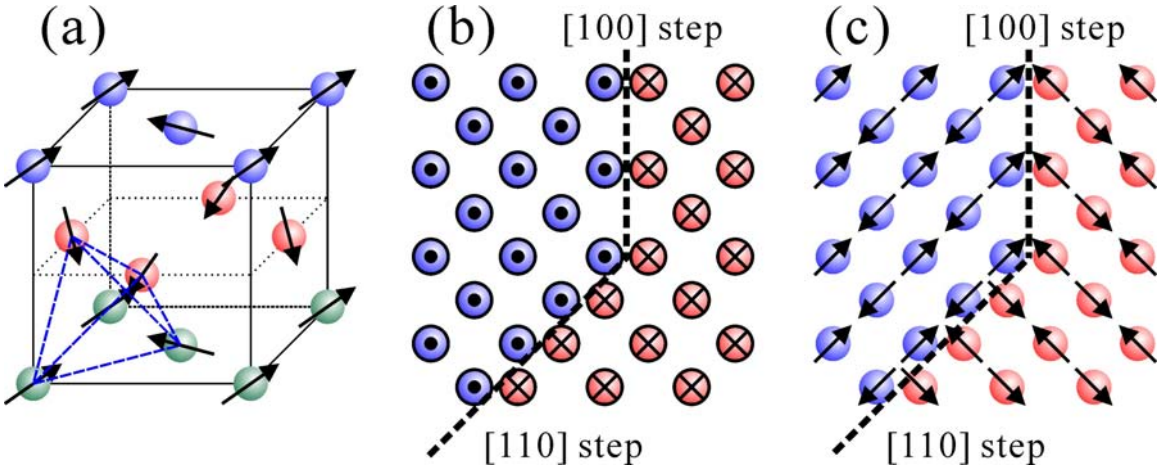


Fig. 5: (color online) (a) the schematic drawing of 3Q-like FeMn spin structure. Arrows represent the spin orientation. Atoms are painted in three different colors to indicate different (001) planes. The dashed lines in (a) show the tetrahedral unit cell. (b) The out-of-plane and (c) in-plane FeMn spin components at a (001) island with [100] and [110] steps. The net out-of-plane spin component is non zero but alternates its direction between neighboring terraces (indicated by dot and cross at the center of atoms). The in-plane spin component has a non zero net spin only at the [100]-type step edges.

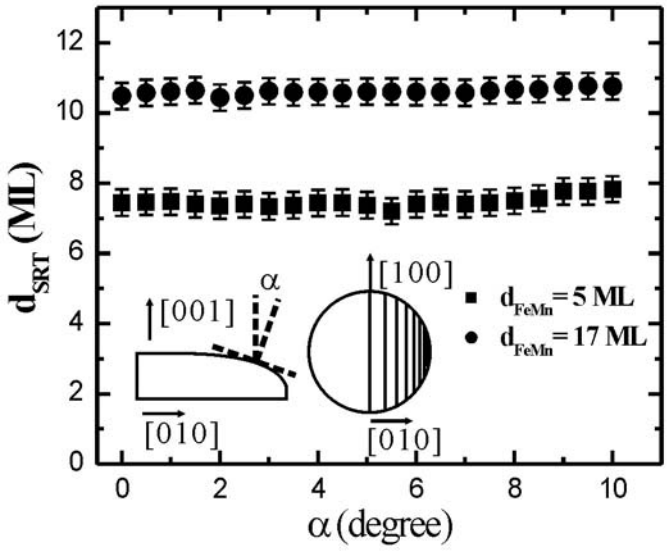


Fig. 6: The Ni SRT thickness $d_{SRT}$ of FeMn/Ni/Cu(001) as a function of the vicinal angle $\alpha$ for $d_{FeMn}$ = 5 ML and 17 ML of FeMn/Ni grown on vicinal Cu(001) with steps parallel to [100].

**References:**


1. S. A. Wolf, D. D. Awschalom, R. A. Buhrman, J. M. Daughton, S. von Molnár, M. L. Roukes, A. Y. Chtchelkanova, and D. M. Treger, Science **294**, 1488 (2001).
2. G. Salls, Y. Kato, K. Enssilin, D. C. Driscoll, A. Gossard, and D. D. Awschalom, Nature **414**, 619 (2001).
3. D. Chiba, M. Sawicki, Y. Nishitani, Y. Nakatani, F. Matsukura, and H. Ohno, Nature **455**, 515 (2008).
4. J. Slonczewski, J. Magn. Magn. Mater. **247**, 324 (2002).
5. E.B. Myers, D.C. Ralph, J.A. Katine, R.N. Louie, and R.A. Buhrman, Science **285**, 867 (1999).
6. T. Zhao, A. Scholl, F. Zavaliche, K. Lee, M. Barry, A. Doran, M. P. Cruz, Y. H. Chu, C. Ederer, N. A. Spaldin, R. R. Das, D. M. Kim, S. H. Baek, C. B. Eom, and R. Ramesh, Nature Materials **5**, 823 (2006).
7. U. Gradmann, J. Korecki, and G. Waller, Appl. Phys. A **39**, 101-108 (1986).
8. J. Chen and J. Erskine, Phys. Rev. Lett. **68**, 1212 (1992).
9. R. K. Kawakami, Ernesto J. Escorcia-Aparicio, and Z. Q. Qiu, Phys. Rev. Lett. **77**, 2570 (1996).
10. P. J. Jensen, K. H. Bennemann, P. Poulopoulos, M. Farle, F. Wilhelm, and K. Baberschke, Phys. Rev. B **60**, 14994 (1999).
11. K. Lenz, S. Zander, and W. Kuch, Phys. Rev. Lett. **60**, 237201 (2007).
12. R. K. Kawakami, M. O. Bowen, Hyuk J, Choi, Ernesto J. Escorcia-Aparicio, and Z. Q. Qiu, Phys. Rev. B **58**, 5924 (1998).
13. J. Choi, J. Wu, C. Won, Y. Z. Wu, A. Scholl, A. Doran, T. Owens, and Z. Q. Qiu, Phys. Rev. Lett. **98**, 207205 (2007).
14. B. Schulz and K. Baberschke, Phys. Rev. B **50**, 13467 (1994).
15. H. W. Zhao, Y. Z. Wu, C. Won, F. Toyoma, and Z. Q. Qiu, Phys. Rev. B **66**, 104402 (2002).
16. W. Kuch, F. Offi, L. I. Chelaru, M. Kotsugi, K. Fukumoto, and J. Kirschner, Phys. Rev. B **65**, 140408 (2002).
17. C. Won, Y. Z. Wu, H. W. Zhao, A. Scholl, A. Doran, W. Kim, T. L. Owens, X. F. Jin, and Z. Q. Qiu, Phys. Rev. B **71**, 024406 (2005).
18. K. Lenz, S. Zander, and W. Kuch, Phys. Rev. Lett. **98**, 237201 (2007).
19. T. C. Schulthess, W.H. Butler, G.M. Stocks, S. Maat, and G.J. Mankey, J. Appl. Phys. **85**, 4842 (1999).
20. U. Schlickum, N. Janke-Gilman, W. Wulfhekel, and J. Kirschner, Phys. Rev. Lett. **92**, 107203 (2004).
21. J. C. Slonczewski, Phys. Rev. Lett. **67**, 3172 (1991).
22. N. C. Koon, Phys. Rev. Lett. **78**, 4865 (1997).

23. R. Jungblut, R. Coehoorn, M. Johnson, J. aan de Stegge, and A. Reinders, J. Appl. Phys. **75**, 6659 (1994).
24. J. Choi, J. Wu, Y.Z. Wu, C. Won, A. Scholl, A. Doran, T. Owens, and Z.Q. Qiu, Phys. Rev. B **76**, 054407 (2007).
25. R. K. Kawakami, Ernesto J. Escorcia-Aparicio, and Z. Q. Qiu, Phys. Rev. Lett. **77**, 2570 (1996).